



Expressing variable mass transfer coefficients for gas fermentation in trickle bed reactor

Sambit Dutta, Hariklia N. Gavala, Ioannis V. Skiadas*

Department of Chemical and Biochemical Engineering, Technical University of Denmark, Søltofts Plads 228A, 2800 Kongens Lyngby

ARTICLE INFO

Keywords:

Volumetric mass transfer coefficient
Trickle bed reactor
Dimensionless equation
Syngas biomethanation
Mass transfer dynamic model

ABSTRACT

Gasification of lignocellulosic biomass and syngas biomethanation are promising technologies for producing biomethane. Trickle bed reactors (TBR) are efficient for syngas fermentation allowing for higher concentration of microbial cells and high surface area for mass transfer. Optimized scaling up and dimensioning of the reactor is crucial when it comes to industrial applications. The first step towards this goal and the scope of the present study is to develop a model able to simulate the mass transfer of gases to the liquid phase as a function of the operating conditions and reactor geometry. Experiments were performed in a lab scale TBR with co-current flow of syngas and water, representing the growth medium, to determine the volumetric mass transfer coefficient ($k_L a$) of each gas compound and its dependence on the flowrate of syngas and water and reactor structural characteristics. The $k_L a$ achieved were in the range of 6.18–13.6 hr^{-1} for H_2 , 2.6–5.79 hr^{-1} for CO and 1.53–3.43 hr^{-1} for CO_2 . A dimensionless equation was fitted to the experimental data and a model was developed to predict $k_L a$ of a specific gas at various gas and liquid flowrates, and reactor configurations. A kinetic model was also developed to simulate the concentrations of syngas in gas phase and liquid phase by applying the $k_L a$ values predicted by the dimensionless correlation. Finally, the model was validated using experimental data obtained by mass transfer coefficient determination in pilot scale TBR with pure argon gas and literature data where the predicted $k_L a$ had a coefficient of variance of $\pm 15\%$ and $\pm 25\%$ respectively within a realistic range of liquid and gas flowrates.

1. Introduction

Gasification of lignocellulosic and other residual biomass is an emerging technology that has been gaining attention due to its ability to convert biomass carbon into a wide range of products [1]. One of the promising products is biomethane, which has the potential to replace fossil derived natural gas in the global gas grid [2]. This is particularly important given the current need to reduce greenhouse gas emissions and mitigate the impact of climate change. The process of producing biomethane involves the conversion of syngas, a mixture of H_2 , CO and CO_2 produced from biomass gasification, into methane through a process known as syngas fermentation. This process has already reached a Technology Readiness Level (TRL) of 4–5 using an efficient trickle bed bioreactor (TBR) based on mixed microbial cultures [3]. The technology has shown promise in efficiently transforming syngas into methane and other valuable liquid products such as alcohols and organic acids [1]. TBR offers several advantages over other reactor types, making them a more efficient option for syngas biomethanation. Primarily, TBR has a

high surface area-to-volume ratio, which facilitates efficient mass transfer of gaseous substrates from the gas phase to the liquid phase [4–6]. This is because the TBR is packed with small-sized particles, which create a large surface area for contact between the gas and liquid phases. This high surface area promotes effective contact between the microbial cultures responsible for biomethanation and the gaseous substrates, leading to efficient and fast conversion of syngas to biomethane [7–9]. Finally, co-current TBR is more resistant to liquid flooding and has improved liquid distribution [10]. The high surface area of the packing material in the TBR promotes effective mixing of the liquid and gas phases, which enhances the availability of gases to the immobilized methanogenic microbial consortia on the packing material [11] and higher productivity of biomethane.

The potential of biomethane as a sustainable and renewable source of energy is enormous, and syngas fermentation offers a promising avenue for its production from lignocellulosic biomass [12]. While the technology has already demonstrated significant progress in lab- and pre-pilot scale experiments, there is still a need to optimize the process

* Corresponding author.

E-mail address: ivsk@kt.dtu.dk (I.V. Skiadas).

<https://doi.org/10.1016/j.cej.2023.146086>

Received 23 June 2023; Received in revised form 21 August 2023; Accepted 14 September 2023

Available online 17 September 2023

1385-8947/© 2023 The Authors. Published by Elsevier B.V. This is an open access article under the CC BY license (<http://creativecommons.org/licenses/by/4.0/>).

and scale up to pilot and commercial scales for continuous operations [3,13]. However, the challenge in optimizing, modeling, and scaling up TBR lies in adequately simulating the mixing of liquid and gas inside the reactor and the mass transfer of gaseous substrates from gas to liquid phase. The mass transfer coefficient influences the rate at which reactants (syngas) are transported from the gas phase to the liquid phase. A greater $k_L a$ value typically leads to improved reactor performance by increasing substrate availability to the microbes and thereby increasing the rate of reaction and improving the efficiency of utilization of syngas [14]. Thus, mass transfer determination is crucial in ensuring efficient conversion of syngas to biomethane, as it facilitates the distribution of gaseous substrates and nutrients to the microbial cultures responsible for the conversion process [15]. In some instances, mass transfer can limit the overall reaction rate, especially if the contact between the gas phase and liquid phase is insufficient [16]. Hence, understanding the mass transfer characteristics is critical for anticipating how the reactor will behave at a bigger scale and different operating conditions to avoid suboptimal performance. Variable $k_L a$ determination allows for more precise inclusion of mass transfer effects into biotic (including microbial growth and biofilm formation) kinetic models that can be used for process simulations, optimal reactor design as well as scaling up from lab scale to pilot and industrial scale. In addition, kinetic models that include variable $k_L a$ can predict the behavior of the reactor under various operating conditions accurately and therefore can be used for optimization of the process for specific products. Research efforts are underway to address this challenge through advanced modeling techniques and experimentation. For instance, computational fluid dynamics (CFD) simulations have been used to model the mass transfer and mixing processes in TBR, while experiments have been conducted to validate the model predictions [17]. Additionally, alternative reactor designs, such as fluidized bed reactors and membrane bioreactors, have been proposed as potential solutions to improve the efficiency of syngas fermentation for biomethane production [6,18]. Another hindrance towards scaling-up of syngas biomethanation is the economic viability of the process. Studies have revealed that operational cost can be reduced almost 15 times by reducing the recirculation rate of liquid from 1500 ml/min to 500 ml/min during syngas fermentation without affecting the conversion efficiency of syngas and productivity of methane [19]. Another approach to reduce the production cost of methane could be intermittent liquid recirculation [20,21]. Studies have shown that periodic liquid recirculation improved the content of methane in outflow gas by 15% and productivity of methane by 5–20 % [22,23].

From the literature survey, it is evident that syngas biomethanation provides a promising alternative for biofuel production and TBR has several operational advantages to support syngas biomethanation on the lab scale [6,24]. Advantages include microbial growth in biofilm which enhances the cell density as TBR have high surface-to-volume ratio, enhanced mass transfer rate compared to stirred tank reactor or bubble column reactor, increased cell retention time in the reactor and high substrate conversion [25–28]. Nevertheless, significant challenges still exist regarding the optimization of the biomethanation process as well as optimization of the scaling up of TBR for continuous operation. The present work focuses on the determination of the volumetric mass transfer coefficient of gases in a trickle bed reactor. The volumetric mass transfer coefficient from gaseous phase to liquid phase and its dependence on the operating and structural characteristics of the reactor is an important aspect of design and operation of a TBR, as it affects the growth pattern of microbes, which constitute the core of the process [29]. Therefore, it is essential to determine the volumetric mass transfer coefficient of a TBR and simulate its variability with the operating conditions and structural characteristic of the reactor to optimize its efficiency for syngas fermentation and biomethane production. The volumetric mass transfer coefficient is a measure of how efficiently gaseous substrates are transferred from the gas phase to the liquid phase and it is also affected by the gas and liquid flowrates and reactor geometry [30,31]. Therefore, determining the volumetric mass transfer

coefficient is crucial in understanding the rate of conversion of syngas to biomethane, as it provides insight into the effectiveness of mass transfer and how to optimize it for efficient biomethane production. Also, by determining the mass transfer coefficient of a TBR, it is possible to optimize the reactor design for conversion of syngas to biomethane. This includes optimum selection of the packing material, liquid and gas flow rates, reactor size and height-to-diameter ratio, and other parameters that affect mass transfer and microbial growth. This optimization can lead to higher conversion rates, lower production costs, and more sustainable production of biomethane. In addition, mass transfer coefficient determination is an important step for scaling up the TBR from lab-scale to pilot-scale or commercial-scale production. This ensures that the optimum parameters are applied consistently across all scales, leading to efficient and sustainable production of biomethane. There are different techniques to experimentally determine concentration of a gas dissolved in a liquid. Some of these techniques include direct measurement of dissolved gases by amperometric sensors [32,33], steady state measurement of gas concentration by oxygen absorption–desorption [34], and offline determination of gas concentration by myoglobin protein method [25]. However, we based our analytical work for the determination of dissolved gas concentration on the method described in Grimalt-Aleman et al. [35]. In the present study, experiments were carried out to determine the volumetric mass transfer coefficient for CO, H₂ and CO₂ in a trickle bed reactor with co-current gas and liquid flow. A dimensionless correlation of the coefficient with the operating conditions and structural characteristics of the reactor was further developed, to predict mass transfer coefficient of the three gases in the liquid phase at different gas and liquid flow rates in a trickle bed reactor. Subsequently, variable mass transfer rate as expressed by the dimensionless correlation was inserted into a kinetic model that included carbon dioxide dissociation in the liquid medium and the model was used to simulate the experimental data obtained from the mass transfer experiments. As discussed earlier, the gas–liquid mass transfer greatly influences the overall reactor performance in syngas biomethanation and hence, estimating variable $k_L a$ values using the dimensionless correlation eliminates the need of experimental determination under different operating conditions and reactor size and geometry which is challenging and time-consuming. Most importantly, after validating the correlation, it can be utilized to predict $k_L a$ of a pure gas or a specific gas component of a gas mixture in a TBR at different gas and liquid flow conditions and different reactor geometry and packing materials and thereby, it can be used as a tool for optimizing process efficiency and scaling up of the reactor. In the present study, a kinetic model accounting for CO₂ dissociation and including variable mass transfer rates as expressed by the dimensionless correlation was developed and used to simulate the gas–liquid mass transfer in the TBR and to predict the concentration of gas in the gas phase and liquid phase of the reactor. Validation of the model was performed based on experimental data obtained with argon, Ar, as well as on literature data. Finally, the methodology presented in this work can be applied and adjusted to several reactor types that are of interest for syngas biological conversions.

2. Materials and methods

A lab scale TBR with a bed volume of 220 ml and a pilot scale TBR with a bed volume of 5000 ml was used in this study. The lab- and pilot scale TBR were set-up as described in Asimakopoulos et al. [3,5]. The height-to-diameter ratio for the lab scale TBR was 7.5 and for the pilot scale was 18.75. Both TBRs were packed with polypropylene/polyethylene packing material (BioFLO 9-Smoky Mountain Biomedia, USA). For the lab scale, the syngas was fed from a 50 l syngas cylinder (Air Liquide) with a composition of 45% H₂, 20% CO, 25% CO₂ and 10 % N₂ and the syngas flowrate was controlled by a mass flow controller (Bronkhorst). The liquid was fed from the top of the reactor using a peristaltic pump (Watson Marlow) and the temperature was controlled using a water bath (VWR). For the pilot scale, the pure argon gas (Ar ≥

99.999%) was fed from a 50 l argon cylinder (Air Liquide) and the argon flowrate was controlled by a mass flow controller (Bronkhorst). Like the lab scale, the liquid was fed from the top of pilot reactor using a peristaltic pump (Watson Marlow) and the temperature was controlled using a water bath (Wittmann). For both lab and pilot TBR, the hot water was recirculated through the jacket around the TBR column from the water bath. Also, for both TBR, there was no liquid recirculation from bottom to the top of the reactor during the experiments. Both gas and liquid samples were taken anaerobically from the outlet of the TBR using a sampling port (Bioprocess Control Instruments).

2.1. Determination of bed porosity

The porosity of lab scale and pilot scale TBRs was determined by the water displacement method. The polypropylene/polyethylene packing material (BioFLO 9-Smoky Mountain Biomedica, USA) was packed inside a measuring cylinder of a volume equal to the volume of the TBR (220 ml for the lab-scale and 5000 ml for the pilot-scale) and water was poured into it. The porosity of the bed was calculated by dividing the volume of water required to fill the packed measuring cylinder by the total volume of the cylinder.

2.2. Volumetric mass transfer experiments

Volumetric mass transfer experiments were conducted in a lab-scale TBR (Fig. 1) using a syngas mixture (H_2 : 45%, CO : 20%, CO_2 : 25% and N_2 : 10%) and distilled water as liquid phase to determine the transfer rate of gas molecules from gas phase to liquid phase by following the two-film theory [36]. The reactor operating temperature was maintained at 60 °C throughout the experiment which is the optimum temperature for methane production by syngas fermentation [4]. Prior to the introduction of syngas and water, the reactor was initially flushed with nitrogen gas for 10 to 15 min, with no flow of syngas and water. After the initial flushing, syngas and water were continuously

introduced at the top of the reactor at the volumetric flow rates indicated in Table 1. The gas and liquid flowrates used for this experiment was taken from previous work [4] and are the flowrates the system have demonstrated maximum conversion of syngas to methane and maximum methane productivity. For simplicity, there was no liquid recirculation but average recirculation rates by previous study were used as resulting equivalent continuous liquid flowrate (See Supplementary Material for detailed calculation in Section S1 and Table S1). Gas and liquid samples were collected from the bottom of the reactor every 60 min for a duration of 4 h. Duplicate experiments were performed for each set of gas and liquid flow rate to determine the volumetric mass transfer coefficient ($k_L a$) of H_2 , CO , and CO_2 . The liquid working volume in the TBR was experimentally determined after each experiment by stopping the liquid flow in the top of the reactor and then collecting the liquid trickling down in a measuring cylinder placed at the bottom of the reactor. During this procedure pure nitrogen gas ($N_2 \geq 99.995\%$) (Air Liquide) was fed from the top of the reactor with a flowrate of 20 ml/min to collect all the trapped water between the packing material (See Supplementary Material for further details in Section S2). The liquid samples, with a volume of 8 ml, were transferred to anaerobic serum vials with a total volume capacity of 11 ml ($\pm 0.75\%$) and subjected to heating at 100°C for a duration of 30 min. The gas components (H_2 , CO and CO_2) were thus transferred out of the liquid to the gas phase. A 100

Table 1

Experimental conditions for mass transfer experiments in lab scale TBR.

Experiment no.	Gas flow rate (ml/min)	Liquid flow rate (ml/min)
1	6.11	24.5
2	6.11	8.25
3	6.11	3.4
4	3.7	24.5
5	3.7	8.25
6	3.7	3.4

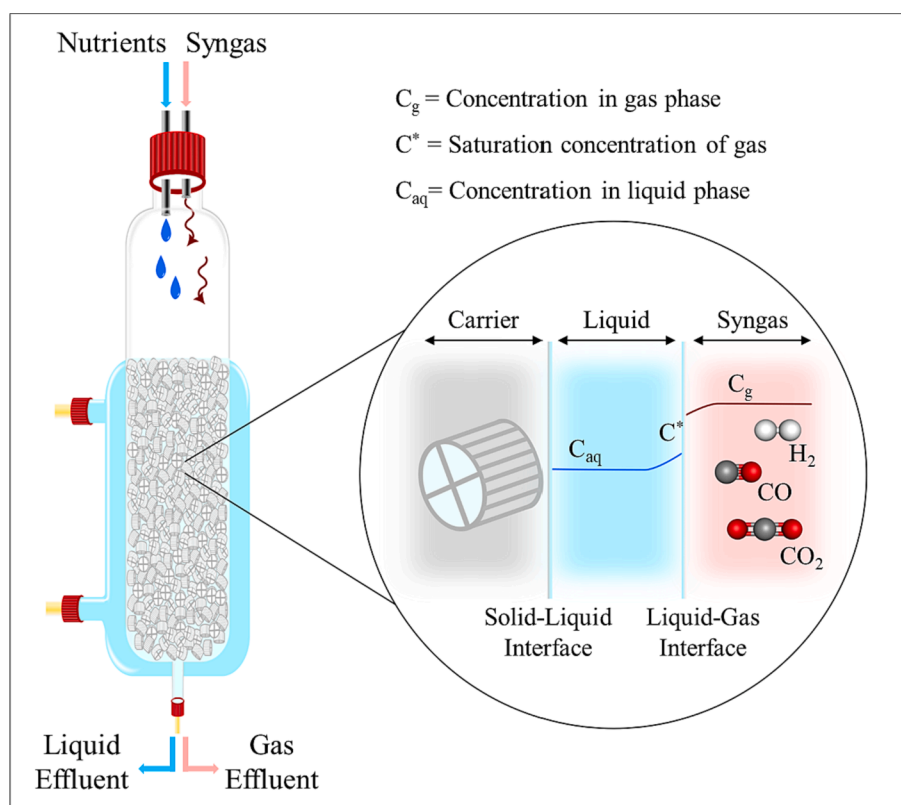


Fig. 1. Illustration of volumetric mass transfer in lab scale trickle bed reactor for co-current flow of gas and liquid from the top of reactor.

μL gas sample was then extracted using a gas-tight syringe to determine the composition of the liquid phase in gaseous components according to the methodology described in Grimalt-Alemany et al. [35]. The calculations to determine the concentration of gas in liquid from analysis of this gas sample is provided in [Supplementary Material](#) (Section S3). Gas samples (100 μL) were also taken from the bottom of the reactor using a gas-tight syringe to determine the composition of gas flowing out of the reactor. These samples were analyzed to determine the concentration of H_2 , CO , and CO_2 in the gas phase. Overall, this experimental procedure aimed to investigate the mass transfer coefficient of H_2 , CO , and CO_2 in a gas-liquid system using a syngas mixture as the gas. The obtained mass transfer coefficient values were used to calculate the rate at which the gas components are transferred from the gas phase to the liquid phase, which can be a critical parameter of syngas biological conversions in TBR. As mass transfer coefficient depends on several factors, a dimensionless correlation (Eq. 4) consisting of terms representing physical properties of both liquid and gas along with physical properties of TBR i.e., porosity of bed, size of packing and dimension of reactor was used to express the dependence of the $k_L a$ on these properties [31]. The dimensionless equation was fitted to experimental data to estimate the parameters or exponents of the dimensionless terms using the function *fitnlm* in MATLAB. To validate the dimensionless equation from lab scale TBR, similar mass transfer experiments were conducted in active pilot scale TBR with Argon gas (See [Supplementary Material](#) for further details in [Table S2](#)). Active pilot TBR means that TBR with active biofilm fermenting syngas to methane. A kinetic model of transfer of gas components from gas phase to liquid phase was executed in Aquasim 2.1 g, as a gas compartment and a mixed liquid compartment with a constant volume linked by a diffusive link [37]. The kinetic model was built using Eq. (1) – (8), where the diffusive link was represented by Eq. (1) and the rate equations were represented by Eq. (5), (6) and (8). The dynamics of CO_2 dissociation was included in the kinetic model as described in Eq. (5). It was assumed that the rate of acid dissociation was very fast [38]. The equilibrium equation for dissociation of water and hydrogen ion was included in the kinetic model as described in Eq. (6) and (8) respectively. It was also assumed that void volume of the reactor is occupied by the gas i.e., volume of the gas compartment has the same volume as void volume. The void volume is obtained by subtracting the total working volume of the TBR from the liquid working volume of the reactor. Both the liquid and gas compartments are assumed to have complete mixing.

2.3. Theoretical calculations

The volumetric mass transfer coefficient of a specific gas ($(k_L a)_g$) is given by Eq. (1) where $Q_{\text{in},g}$ and $Q_{\text{out},g}$ are the molar inflow and outflow of the gas, respectively, V_L is the liquid working volume inside the reactor and C_g^* and $C_{\text{aq},g}$ are the saturation concentration of gas in liquid phase and the actual concentration of gas in liquid phase, respectively.

$$(k_L a)_g = (Q_{\text{in},g} - Q_{\text{out},g}) / V_L (C_g^* - C_{\text{aq},g}) \quad 1$$

The saturation concentration of the gas (C_g^*) is calculated by applying Henry's law (Eq. 2) where C_g is the concentration of gas in the gas phase.

$$C_g^* = K_H^* C_g \quad 2$$

Temperature correction for Henry's constant (K_H) was done using Van't Hoff equation (Eq. 3) where $-\Delta H^\circ$ is the standard enthalpy of solution of a specific gas as found in Alberty [39] and Haynes [40].

$$K_H = K_H^\circ \exp\left(\frac{-\Delta H^\circ}{R} \left(\frac{1}{T} - \frac{1}{T^\circ}\right)\right) \quad 3$$

A dimensionless correlation was used to express the mass transfer coefficient for a gas compound ($(k_L a)_g$) in a gas mixture, and it is given in Eq. (4) [31]. It includes dimensionless terms for gas properties (X_G and

Sc_L), and liquid properties (X_G , Re_L , We_L and Sc_L) and a dimensionless term for reactor configuration (θ). The exponents of the dimensionless terms i.e., a, b, c, d, and e were estimated using MATLAB. In the present work, water was used as the liquid and syngas comprising 45% H_2 , 20% CO , 25% CO_2 and 10 % N_2 in molar fraction was used as the gas mixture.

$$Sh_{L,g} = \Omega^* X_G^{a*} Re_L^{b*} We_L^{c*} Sc_L^{d*} \theta^e \quad 4$$

For the kinetic model in Aquasim, the acid-base equilibrium equation (Eq. 5) was included to describe the kinetics of CO_2 dissociation, where K_{CO_2} is the dissociation constant of CO_2 , and C_{CO_2} and $C_{\text{HCO}_3^-}$ are the concentration of CO_2 and HCO_3^- in liquid respectively.

$$K_{\text{CO}_2/\text{HCO}_3^-} = \left(C_{\text{CO}_2} - \frac{C_{\text{HCO}_3^-} * C_{\text{H}^+}}{K_{\text{CO}_2}} \right) \quad 5$$

The equilibrium equation for water (Eq. 6) was also included to describe the kinetics of water dissociation, where $K_{\text{H}_2\text{O}}$ is the dissociation constant of H_2O , and C_{H^+} and C_{OH^-} are the concentration of hydrogen and hydroxyl ions respectively.

$$C_{\text{OH}^-} - \frac{K_{\text{H}_2\text{O}}}{C_{\text{H}^+}} = 0 \quad 6$$

Temperature correction for K_a was done using Eq. (7), where a is CO_2 for Eq. (5) and H_2O for Eq. (6), and $-\Delta H^\circ$ is the standard enthalpy of reaction as found in Alberty [39].

$$K_a = K_a^0 \exp\left(\frac{-\Delta H^\circ}{R} \left(\frac{1}{T} - \frac{1}{T^\circ}\right)\right) \quad 7$$

Finally, an equilibrium equation for C_{H^+} ion was also included in kinetic model which is shown in Eq. (8)

$$C_{\text{H}^+} - C_{\text{HCO}_3^-} - C_{\text{OH}^-} = 0 \quad 8$$

3. Analytical methods

For gas mixture samples, the content (mol %) of H_2 , CO and CO_2 were determined using gas chromatography. An SRI 8610C chromatograph was equipped with a Molsieve 13x column followed by a silica gel column. The flow of gas towards any of the two columns was controlled by a rotating valve. Gas samples of 100 μL (SGE 1MR-VLL-GT gas tight syringe by Mirkolab Aarhus A/S) were injected and Helium was used as the carrier gas at a flowrate of 50 ml/min. The column temperature was kept constant for 3 min at 65 °C and then it was increased by 10 °C/min up to 95 °C. Then the rotating valve changed the gas flow towards silica gel column followed by a temperature ramp of 24 °C/min up to 140 °C [5]. The relative standard deviation of the gas measurements is $\pm 0.5\%$.

4. Results and discussions

4.1. Bed porosity of TBR

Using the water displacement method, the porosity of the bed was found to be 0.79 in the lab scale TBR and 0.78 in the pilot scale TBR.

4.2. Mass transfer experiments

Estimating the volumetric mass transfer coefficients ($k_L a$) of gases in a liquid medium and combining it with microbial growth kinetics is important for determining product formation rates. However, it can be challenging to accurately determine $k_L a$ coefficients due to potential biological activity that could interfere with the measurement process. To overcome this challenge, abiotic experiments were conducted at a temperature of 60°C to determine the $k_L a$ of all gases. This approach leads to a more accurate estimation of the volumetric mass transfer coefficient [35].

The $k_L a$ of each gas was determined using Eq. (1); and the data used for the calculation of the $k_L a$ values are presented in [Table 3](#). The

average values ($k_L a$) from duplicate experiments are presented in Table 3 and the full result of the mass balance of gas in and out from the TBR and the duplicate $k_L a$ values are presented in the Supplementary Material Table S3 and S4 respectively. The results of the abiotic experiments revealed that the $k_L a$ coefficients for all gases increased as the liquid flow rate decreased at a specific gas flow rate. This is because a decrease in liquid flow rate increased the residence time of the liquid in the TBR, promoting longer contact between gas and liquid phases, and thus an increase in $k_L a$. The findings may also be seen in Fig. 2, which depicts the relationship between liquid flow rate as expressed by the Reynolds number, also shown in Table 3, and $k_L a$ coefficients for all gases. The liquid phase Reynolds number (Re_L) was calculated according to the formula mentioned in Table 2 and using the value of the superficial velocity of the liquid (v_L) from Table 3. Additionally, the results showed that reducing the gas flow rate resulted in a decrement of the concentration gradient between the gas and liquid phases, thereby decreasing the driving force of mass transfer and lowering the $k_L a$ [48]. This underscores the importance of carefully controlling the liquid and gas flow rates during bioprocess engineering to optimize microbial growth and product formation. It is worth noting that the accurate determination of $k_L a$ coefficients is crucial in enhancing bioprocess performance. According to some studies the ratio of mass transfer coefficient of pure gas a over pure gas b is proportional to the square root of ratio of their diffusivity [49,50]. Such as ratio of $k_L a$ of H_2 over $k_L a$ of CO is proportional to the square root of diffusivity of pure H_2 over diffusivity of pure CO. Results shows that $k_L a$ ratio is proportional to the square root of diffusivity of pure gas i.e., as the ratio of $k_L a$ for gases increases, the diffusivity ratio of pure gas also increases. In the present study gas mixture (syngas) and not pure gas was used for mass transfer experiments and hence, there is a correction to the diffusivity of the pure gas which is represented as effective diffusivity. Therefore, the results showed that the ratio of $k_L a$ for gases increases as the effective diffusivity ratio decreases i.e., the $k_L a$ ratio is inversely proportional to the square root of effective diffusivity of the gas in syngas mixture (See Supplementary Material for further details in Table S5 and S6). The values of $k_L a$ coefficients are used in mathematical models to simulate the behavior of bioprocesses, which enables researchers to understand and optimize the processes. Furthermore, the determination of $k_L a$ coefficients allows researchers to predict the impact of changing operating conditions, which can be used to optimize bioprocess performance. Ultimately, accurate determination of $k_L a$ coefficients is essential for enhancing bioprocess performance and improving our understanding of bioprocess behavior.

Empirical correlations are often utilized to predict the volumetric mass transfer coefficient in various types of reactors. One such reactor is the trickle bed reactor, for which literature provides the correlation of $k_L a$ with several dimensionless numbers as explained in section 2.3. In the present study, Eq. (4) was used to fit the experimentally obtained $k_L a$ and estimate the parameters a, b, d, and e [30,31,51,52]. Due to the crucial influence of surface tension effects on the rate of mass transfer

from gas to liquid, the exponent of We_L , denoted as c, was assumed to be one. This is because the specific surface area of packing material directly influences the surface tension of liquid. In the case of TBR, the liquid flows through the channels between the packing and passage of liquid through the channels is governed by capillary phenomena where the surface tension of liquid plays a substantial role on how strongly the liquid molecules are attracted to each other and to the packing material [53,54]. Thus, in high surface area packing materials, capillary phenomena become prominent as the number of channels for liquid flow decrease, and surface tension becomes fundamental in determining the effective surface area available for mass transfer [55]. The result of parameter estimation from the nonlinear fitting of Eq. (4) to the experimentally determined $k_L a$ values is presented in Table 4. The table shows that the standard error (SE) for all parameters is less than 0.05, indicating minimal deviation of estimated parameter from its true value. The large t-statistic (tStat) suggests that all four estimated parameters are statistically significant and far from the null hypothesis value. The null hypothesis can be rejected as the p-value (pValue) of the estimated parameters is less than 0.05, indicating their statistical significance. The model fitting of Eq. (4) resulted in an adjusted R^2 value of 0.99 which suggests that the model fits the experimental data accurately, and F-statistic vs zero model value of 9330 with a pValue of $8.32E-24$ indicates the model fits the data compared to the null model, with a low pValue, providing strong evidence in favor of the fitted model. Fig. 3 illustrates the variation of experimental values and model-predicted values of $k_L a$ with Re_L at syngas flow rates of 6.11 ml/min and 3.7 ml/min. It may be seen that the model accurately fits all three gases, with an R^2 value greater than 0.99 for each of them. In summary, empirical correlations are widely used to predict the volumetric mass transfer coefficient in different types of reactors, and Eq. (4) is commonly used to estimate $k_L a$ in trickle bed reactors. The estimated parameters (a, b, d, and e) from the nonlinear fitting of Eq. (4) were statistically significant and accurately fit the experimental data. The results provide useful insights into the mass transfer phenomena in a trickle bed reactor, which can be beneficial in reactor design and optimization. The equation obtained to predict the $k_L a$ at different gas and liquid flowrates and different reactor geometry is given below:

$$(k_L a)_g = \frac{D_{eff,L,g}}{d_h^2} * \Omega * X_G^{0.7436} * Re_L^{-1.444} * We_L^1 * Sc_L^{3.2919} * \theta^{2.0977} \quad 9$$

Several studies have been conducted to determine volumetric mass transfer coefficient in various reactor types and different operating conditions. Since mass transfer coefficient depends on several factors such as working volume of the reactor, flowrate of the gas etc., a dimensionless factor ω , calculated as the working volume of the reactor over the product of the flowrate of gas with $k_L a$, is used as a tool to compare gas-liquid mass transfer of different reactor configurations and gas flow rates. A comparative assessment of volumetric mass transfer coefficient with existing literature is shown in Table 5. From the table we can observe that, ω for CO in the present study is in between 2.5 and

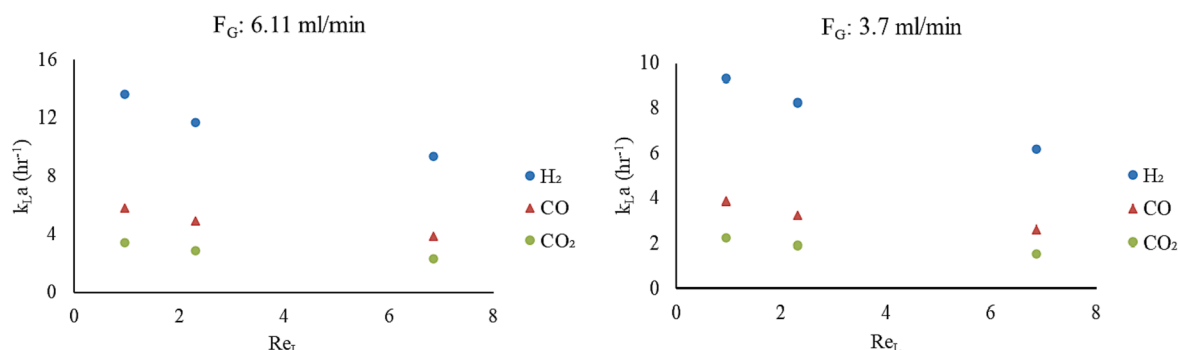


Fig. 2. Variation of mass transfer coefficient ($k_L a$) of H_2 , CO and CO_2 with Reynolds number for liquid (Re_L) at gas flowrates F_G : 6.11 ml/min and 3.7 ml/min.

Table 2

Terms, variables, and values for Eq. (4).

Abbreviation	Name	Value	Description/ Source
Sh _{L,g}	Liquid phase Sherwood number for a specific gas	$\frac{(k_L a)_g d_h^2}{D_{eff,L,g}}$	It is the ratio of convective mass transfer to the rate of diffusive mass transfer.
X _G	Lockhart-Martinelli number for a gas	$\frac{v_G}{v_L} \sqrt{\frac{\rho_L}{\rho_G}}$	It represents the flow of gas in a gas-liquid fluid mixture.
Re _L	Liquid phase Reynolds number	$\frac{v_L \rho_L d_p}{\mu_L}$	It represents the flow conditions of liquid i.e., laminar, transient, or turbulent.
We _L	Liquid phase Weber number	$\frac{v_L^2 \rho_L d_p}{\sigma_L}$	It represents the effect of inertial force and surface tension on the flowing liquid in a system.
Sc _L	Liquid phase Schmidt number	$\frac{\mu_L}{\rho_L D_{eff,L,g}}$	It represents the transport of momentum and mass of liquid in a system.
θ	Dimensionless term for reactor properties	$\frac{a_v d_h}{1 - \varepsilon}$	
d _h	Krischer and Kast hydraulic diameter, m	$d_p \sqrt[3]{\frac{16\varepsilon^3}{9\pi(1 - \varepsilon)^2}}$	
Ω	Cross sectional area of the TBR, m ²	1.257E-03	
ε	Porosity of the TBR	0.79	
d _p	Diameter of packing material, m	0.01	
v _G	Superficial velocity of gas, m/s	$\frac{F_G}{\Omega}$	
v _L	Superficial velocity of liquid, m/s	$\frac{F_L}{\Omega}$	
F _G	Volumetric flowrate of syngas to the reactor, m ³ /s		
F _L	Volumetric flowrate of liquid to the reactor, m ³ /s		
ρ _L	Density of liquid at 60°C, kg/m ³	983.19	[41]
ρ _G	Density of syngas at 60°C, kg/m ³	0.6917	
μ _L	Viscosity of liquid at 60°C, kg/m.s	4.658E-04	[42]
σ _L	Surface tension of liquid at 60°C, kg/s ²	6.62E-02	[43]
a _v	Specific surface area of packing material, m ² /m ³	800	[5]
D _{eff,L,g}	Effective diffusivity of a gas in liquid with the gas being part of a gas mixture, m ² /s	$D_{eff,L,g} = \frac{1 - y_A}{\frac{y_B}{D_{L,gB}} + \frac{y_C}{D_{L,gC}} + \dots}$	[44]

Table 2 (continued)

Abbreviation	Name	Value	Description/ Source
D _{W,H2}	Diffusivity of H ₂ in water at 60°C, m ² /s	1.31E-08	[45]
D _{W,CO}	Diffusivity of CO in water at 60°C, m ² /s	5.68E-09	[46]
D _{W,CO2}	Diffusivity of CO ₂ in water at 60°C, m ² /s	3.80E-09	[47]

3.5 which is higher than ω reported for CO in a stirred tank reactor (STR), packed bed reactor (PBR) and a bubble column reactor (BCR). Only for hollow fiber membrane reactor (HFMBR) ω for CO was significantly higher than the values reported in the present study. Since the present study did not include any recirculation of liquid, we are not comparing the ω values of CO with that reported in Cowger et al. [56]. Very few studies were conducted to develop a dimensionless correlation for volumetric mass transfer coefficient in a trickle bed reactor. The multiphase interaction in TBR can be divided into various flow regimes namely low interaction or trickle flow regime, high interaction or pulse, bubble flow regimes and transition zone. Low interaction is defined by low gas and liquid flowrate and high interaction is defined by high gas and liquid flowrate whereas transition zone is defined by moderate flowrates of liquid and gas [57,58]. The correlations reported in the literature for TBR and micro(μ)PBR along with the correlation from our current study are shown in Table 6. From the table, we can observe that the dimensionless correlation is varying as the flow regime within the TBR changes, and our current study is based on low interaction regime or trickle flow.

4.3. Mass transfer simulations

Following the experimental determination of k_La and developing a dimensionless equation (Eq. 9), a kinetic model was developed to simulate the data obtained from the mass transfer experiments in the TBR. The developed model was used to predict the concentration of gas components in the gas and liquid phase of the TBR. There was an excellent quantitative agreement between the model predictions and the measured concentrations of H₂, CO and CO₂ in the gas and liquid phase of TBR. The kinetic model also exhibited high conformity with all six sets of experimental data, as demonstrated in Fig. 4. Based on the model predictions, the steady state was achieved within one hour for a gas flow rate of 6.11 ml/min and 1.5 h for a gas flow rate of 3.7 ml/min. This implies that higher gas flow rates will result in a faster attainment of steady state in both gas and liquid phases. The agreement between the model predictions and experimental measurements implies that the model can be reliably used to predict concentrations of H₂, CO and CO₂ in the gas phase and liquid phase of TBR. It also validated the dimensionless model for k_La determination which can be used for estimating k_La at different gas and liquid flowrates in a TBR. This provides a more versatile tool for the prediction of mass transfer rates in TBRs and can be used to optimize reactor design and operating conditions for a wide range of applications. Overall, the validation of the model used in this study is crucial for ensuring that the results obtained are reliable and can be used to improve the performance of TBRs. The use of a dimensionless model for k_La is also significant, as it provides a more flexible approach for predicting mass transfer rates in TBRs, which can be useful for process optimization and design.

4.4. Model validation

The dimensionless model was validated by experimental results obtained from mass transfer tests in pilot scale TBR using Argon gas (See

Table 3Volumetric mass transfer coefficient of H₂, CO and CO₂ under different operating conditions.

		Experiments					
		1	2	3	4	5	6
Operating conditions	Syngas flow rate (ml/min)	6.11			3.7		
	Water flow rate (ml/min)	24.5	8.25	3.4	24.5	8.25	3.4
	Superficial velocity of water (m/s)	0.00032	0.00011	4.5E-05	0.00032	0.00011	4.5E-05
Saturation concentrations	C _{H₂} * (mmol/l)	0.291	0.291	0.291	0.291	0.291	0.291
	C _{CO} * (mmol/l)	0.116	0.116	0.116	0.116	0.116	0.116
	C _{CO₂} * (mmol/l)	3.46	3.46	3.46	3.48	3.47	3.46
Measured	C _{aq,H₂} (mmol/l)	0.027	0.069	0.13	0.018	0.05	0.0996
	C _{aq,CO} (mmol/l)	0.005	0.014	0.03	0.0034	0.0098	0.022
	C _{aq,CO₂} (mmol/l)	0.077	0.233	0.537	0.05	0.156	0.3726
Calculated	V _L (l)	0.0163	0.0135	0.0117	0.0163	0.0135	0.0117
	Q _{in,H₂} - Q _{out,H₂} (mmol/min)	0.0006723	0.0005854	0.0004269	0.0004584	0.0004456	0.0003474
	Q _{in,CO} - Q _{out,CO} (mmol/min)	0.0001164	0.0001135	9.722E-05	7.97E-05	7.741E-05	7.146E-05
	Q _{in,CO₂} - Q _{out,CO₂} (mmol/min)	0.0021439	0.0020917	0.0019582	0.0014291	0.0014255	0.0013592
	Re _L	6.85	2.3	0.95	6.85	2.3	0.95
	k _L a _{H₂} (hr ⁻¹)	9.37	11.72	13.6	6.18	8.21	9.3
	k _L a _{CO} (hr ⁻¹)	3.85	4.94	5.79	2.6	3.23	3.89
	k _L a _{CO₂} (hr ⁻¹)	2.33	2.88	3.43	1.53	1.91	2.25

Table 4

Estimated parameter of from non-linear fitting of Eq. (4).

Parameter	Estimated value	Standard Error	tStat	p-value
a	0.7436	0.022088	33.665	8.4825e-15
b	-1.444	0.023098	-62.535	1.5423e-18
d	3.2919	0.042025	78.332	6.6429e-20
e	2.0977	0.049723	42.187	3.7081e-16

Supplementary Material for experimental results in Table S7). The experiments were conducted on an active pilot TBR with active biofilm fermenting syngas to methane. Thus, argon gas was used for mass transfer experiment and not syngas as Ar is not consumed or produced by syngas fermenting microbes and Ar is not toxic for the microbes. Eq. (9) was used to predict the mass transfer coefficient of Argon in water at the experimental conditions, at which the Argon-water mass transfer coefficient was measured in pilot scale TBR. The results are presented in parity plot shown in Fig. 5, where the x-axis represents the k_La predicted by the model and the y-axis represents the k_La obtained by experiments in pilot scale TBR. The parity plot shows that the model-predicted k_La values are in good agreement with the experimentally obtained data from mass transfer experiments in pilot scale TBR. The coefficient of variance, CV, is $\pm 15\%$, which indicates a good fit between experimentally obtained data and model predicted data. Thus, the model can be used to predict the mass transfer coefficient of gas in water for pilot scale TBR and therefore validating that the developed model based on the dimensionless correlation can be applied to different gases and to TBR of different scale and dimensions.

For further validation, the dimensionless model for k_La estimation i. e., Eq. (9) with the estimated parameters (Table 4) was used to predict the volumetric mass transfer coefficient of oxygen in a TBR as

determined and reported by other researchers in the field. Therefore, the k_La values predicted by the model developed in the present study were compared with the k_La values of oxygen experimentally obtained by Orgill et al. [48]. The experiments Orgill et al. performed covered Reynolds' number of gas from 0.01 to 0.56 and Reynolds number of liquid from 1.7 to 24.18. The results are presented in a parity plot shown in Fig. 6, where the x-axis represents the experimentally obtained k_La values [48], and the y-axis represents the model-predicted k_La values. The parity plot shows that the model predicted k_La values are in good agreement with the experimentally obtained data for Reynolds number of liquid (Re_L) less than 15 and Reynolds number of gas (Re_G) less than 1. The coefficient of variance (CV) for this range is $\pm 25\%$, which indicates a good fit between the two variables. The data points are clustered around the diagonal line, indicating that the model is accurately predicting the k_La values. However, for higher Re_L, the CV was greater than 25%, indicating a poor prediction of k_La with respect to experimentally determined values. This may be due to the limitations of the model for predicting k_La at high gas and liquid flowrates. Thus, the dimensionless equation can be used to predict mass transfer coefficient for Re_G less than 1 and Re_L less than 15. Overall, the dimensionless equation for k_La estimation showed promising results in predicting k_La values in a TBR, within certain limitations. Future research can focus on improving the model's accuracy for higher F_G and F_L values, as well as applying the model to other types of reactors and processes.

Thus, the dimensionless correlation can predict the volumetric mass transfer coefficient of gas in water for both lab scale and pilot scale TBRs. The correlation is dependent on the gas and liquid flowrates, physical properties of gas and liquid which is dependent on temperature and pressure, reactor geometry and reactor properties such as porosity of the packed bed and diameter of the packing material. The correlation and kinetic model are based on syngas biomethanation process under

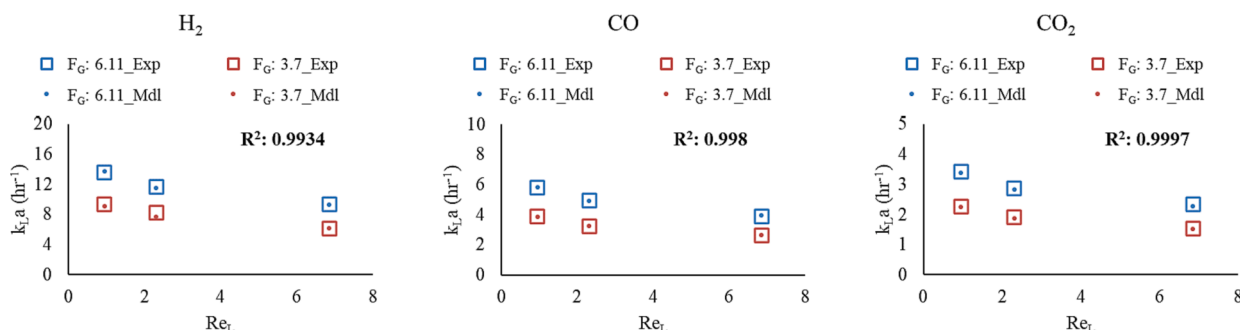
**Fig. 3.** Comparison of experimental (Exp) and Model (Mdl) estimated values of k_La vs Re_L at syngas flowrate (F_G) of 6.11 and 3.7 ml/min.

Table 5

Volumetric mass transfer coefficient values of different gases for different reactor configurations and operating conditions.

Reactor Type	Gas composition	Experimental Parameters				$k_L a$ (h ⁻¹)	ω (V/ F _G *k _L a)	Ref.
		Working volume (V) (l)	Gas flowrate (F _G) (ml/min)	Packing	Agitation			
STR	99.99% CO	7	6000	NA	600 rpm	154.8	3.01	[25]
STR	52 % N ₂ , 20% CO, 18% CO ₂ , and 10% H ₂	5	15,000	NA	700 rpm	288 CO	1.6	[59]
PBR	80% CO and 20% CO ₂	2	29	Polyurethane sponge (1 × 1 × 1 cm ³)	NA	1.63 CO	1.87	[60]
BCR	Air	0.5	400	Sparger: ceramic membrane module (0.2 μm), gas supply area: 75.4 cm ²	NA	163.6	3.4	[26]
BCR	99.99% CO	0.5	400	Sparger: ceramic membrane module (0.2 μm), gas supply area: 75.4 cm ²	NA	113.7	2.36	[26]
BCR	99.99% CO	3	5000	Sparger: column diffuser	NA	40	0.4	[61]
BCR	99.99% CO	3	5000	Sparger: 20 μm bulb diffuser	NA	78.8	0.788	[61]
BCR	99.99% CO	3	5000	Sparger: ring sparger (0.5 μm)	NA	50.4	0.504	[61]
HFMBR	50% CO, 30% H ₂ , and 20% CO ₂	0.13 (HFM), and 2.4 (Reservoir)	35	Hydrophobic polypropylene membrane	NA	21 CO	25.3	[62]
HFMBR	99.99% CO	8	5000	Microporous hydrophobic polypropylene membrane	NA	1096.2	29.23	[63]
TBR	Air	1	130.9	3 mm soda lime glass beads	NA	171	21.772	[48]
TBR	Air	1	106.4	6 mm soda lime glass beads	NA	421	65.946	[48]
TBR	55% CO, 20% H ₂ , 15% Ar, and 10 %CO ₂	1	10	6 mm ceramic Intalox saddle, liquid recirculation rate: 100 ml/min	NA	22 CO	36.67	[56]
TBR	55% CO, 20% H ₂ , 15% Ar, and 10 %CO ₂	1	10	6 mm ceramic Intalox saddle, liquid recirculation rate: 240 ml/min	NA	38 CO	63.33	[56]
TBR	Syngas	NA	NA	Ceramic Intalox saddles	NA	55.5		[64]
TBR	45% H ₂ , 25% CO ₂ , 20% CO, and 10 % N ₂	0.22	6.11	BioFLO 9-Smoky Mountain Biomedica, liquid flowrate: 3.4 ml/min	NA	13.6 H ₂ 5.79 CO 3.43 CO ₂	8.161 3.474 2.058	Present study
TBR	45% H ₂ , 25% CO ₂ , 20% CO, and 10 % N ₂	0.22	3.7	BioFLO 9-Smoky Mountain Biomedica, liquid flowrate: 24.5 ml/min	NA	6.18 H ₂ 2.6 CO 1.53 CO ₂	6.124 2.576 1.516	Present study

Table 6

Dimensionless correlations for volumetric mass transfer coefficient in liquid phase for trickle flow or trickle bed reactors.

Reactor Type	Correlations	Ref.
TBR	Low interaction: $(k_L a)_g = \frac{D_{eff,L,g}}{d_h^2} * 2.8 * 10^{-4} * X_G^{0.85} * Re_L^{0.68} * We_L^{0.68} * Sc_L^{1.7} * \theta^{0.85}$	[65]
TBR	High interaction: $(k_L a)_g = \frac{D_{eff,L,g}}{d_h^2} * 0.45 * X_G^{0.65} * Re_L^{1.04} * We_L^{0.26} * Sc_L^{0.65} * \theta^{0.325}$	[65]
TBR	Transition zone: $(k_L a)_g = \frac{D_{eff,L,g}}{d_h^2} * 0.091 * X_G^{0.95} * Re_L^{0.76} * We_L^{0.76} * Sc_L^{1.14} * \theta^{0.95}$	[65]
μPBR	$(k_L a)_g = \frac{D_{eff,L,g}}{d_h^2} * 3.41 * 10^{-5} * X_G^{0.08} * Re_L^{3.1} * We_L^{-1.33}$	[66]
TBR	Trickle flow: $(k_L a)_g = \frac{D_{eff,L,g}}{d_h^2} * 2.87 * 10^{-4} * X_G^{0.4} * Re_L^{0.5} * We_L^{0.38} * Sc_L^{1.7} * \theta^{0.85}$	[67]
TBR	Pulse flow: $(k_L a)_g = \frac{D_{eff,L,g}}{d_h^2} * 1.05 * X_G^{0.5} * Re_L^{0.2} * We_L^{0.35} * Sc_L^{0.65} * \theta^{0.325}$	[67]
TBR	Bubble flow: $(k_L a)_g = \frac{D_{eff,L,g}}{d_h^2} * 9.93 * 10^{-3} * X_G^{0.8} * Re_L^{0.1} * We_L^{-1.2} * Sc_L^{0.65} * \theta^{0.325}$	[67]
TBR	$(k_L a)_g = \frac{D_{eff,L,g}}{d_h^2} * 1.257 * 10^{-3} * X_G^{0.7436} * Re_L^{-1.444} * We_L^1 * Sc_L^{3.2919} * \theta^{2.0977}$	Present study

atmospheric pressure and temperature of 60 °C. Since the model includes the terms representing the physical properties of gas and liquid which is in turn dependent on temperature and pressure, it can be used at different process conditions. This correlation could be used to determine $k_L a$ in real life gas fermentation systems which will help to optimize the process on a larger scale. Further studies can be carried out to fine tune the dimensionless correlation by maintaining a constant pH during the experimental procedure or observing the effect of

temperature on the volumetric mass transfer coefficient.

5. Conclusion

A dimensionless correlation for determining the volumetric mass transfer coefficient of a gas in a liquid in co-current trickle bed reactor was developed. The correlation was a function of gas and liquid flow-rate, physical properties of gas and liquid, reactor geometry and reactor

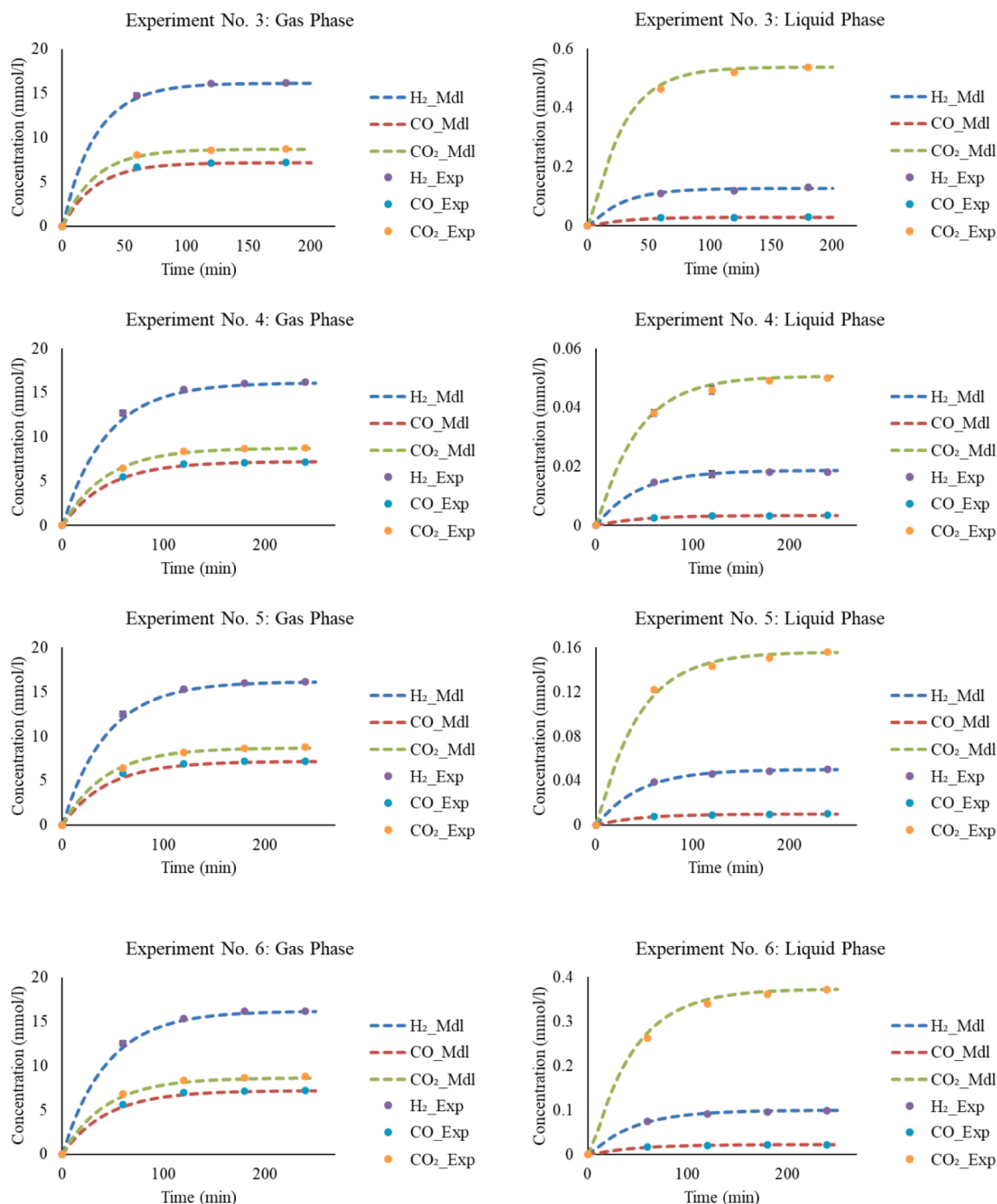


Fig. 4. Comparison of experimental (Exp) and model (Mdl) predicted values of concentration of H₂, CO and CO₂ in gas phase (Gas volume) and liquid phase (Liquid Volume) for TBR for 6 set of experimental data. Due to the numeric values being significantly different we had to use different scales for the vertical axis of some graphs in this figure.

configuration. It can be used to accurately predict the k_{La} values of a pure gas or a gas component in a gas mixture in such a system under different operating conditions and reactor size and geometry. To develop this correlation, experiments were conducted where the volumetric mass transfer coefficient, k_{La} , of H₂, CO and CO₂ in water in lab-scale trickle bed reactor, TBR, with co-current flow of gas and liquid, was determined. The highest mass transfer coefficient of H₂, CO and CO₂ achieved were 13.6 hr⁻¹, 5.79 hr⁻¹, and 3.43 hr⁻¹ respectively at a syngas flowrate of 6.11 ml/min and water flowrate of 3.4 ml/min. At a

constant gas flowrate, k_{La} increases with decrease in liquid flowrate as a decrease in liquid flow rate increases the residence time of the liquid in the TBR, promoting longer contact between gas and liquid phases, and thus an increase in k_{La} . At constant liquid flowrate, k_{La} decreases with decrease in gas flowrate as it results in decrement of the concentration gradient between the gas and liquid phases, thereby decreasing the driving force of mass transfer and lowering the k_{La} . The dimensionless equation was applied to correlate k_{La} with the liquid and gas flowrates, reactor configuration and physical properties of liquid and gas. This

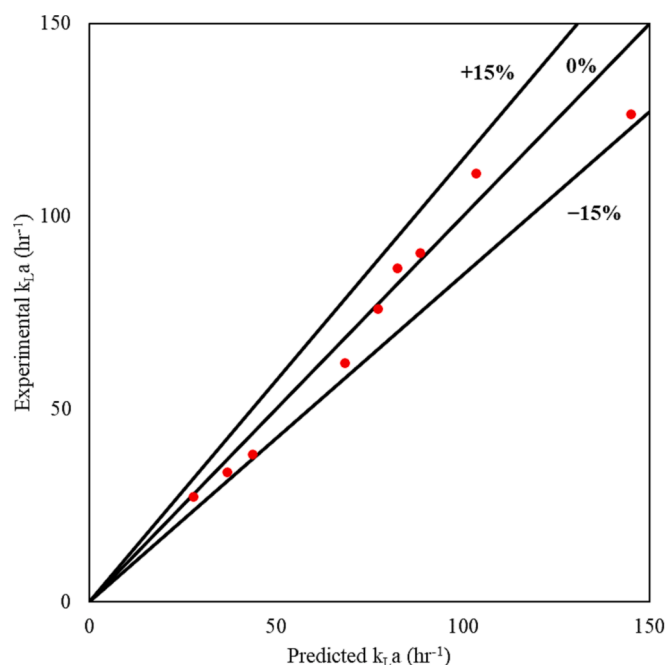


Fig. 5. Comparison of model predicted and experimental values of k_La (hr^{-1}) in pilot scale TBR.

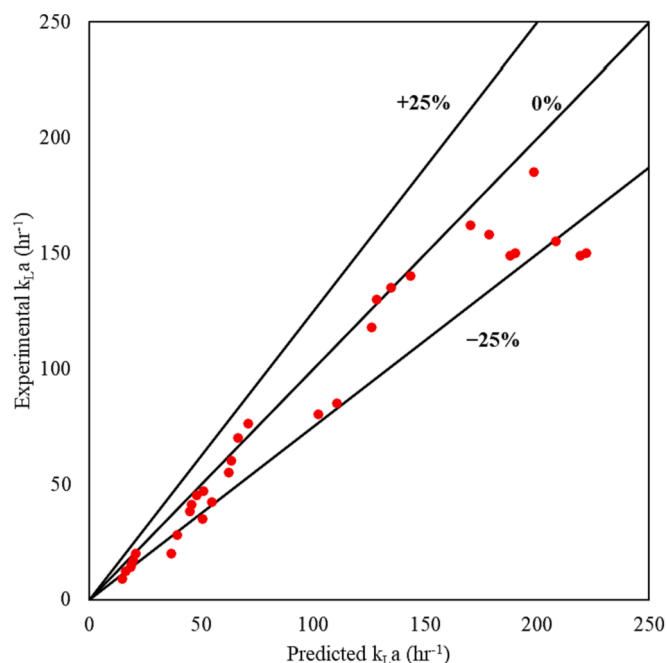


Fig. 6. Comparison of model predicted and experimental values of k_La (hr^{-1}) in lab scale TBR.

equation had an excellent fit with the experimental data with R^2 of 0.99. A kinetic model was further developed to simulate the data obtained from the mass transfer experiments in the lab-scale TBR. The model exhibited high conformity with all experimental data for both gas and liquid phase of the TBR. Subsequently, the dimensionless equation for k_La determination was validated based on k_La data reported in literature as well as experimental data obtained with Argon gas, Ar, in a pilot-scale TBR. All the predicted k_La values were found to lie within $\pm 25\%$ of the respective literature data for liquid Reynolds number, Re_L less than 15 and gas Reynolds number, Re_G less than one. The predicted k_La values

for Ar in the pilot TBR were found to lie within $\pm 15\%$ of k_La calculated from the experimental data. Thus, the developed model based on the dimensionless correlation can be used for simulating variable mass transfer rates of gas components in a TBR. In summary, in the present study, a model was developed that can predict the volumetric mass transfer coefficient and consequently the mass transfer rate of gas components in a trickle bed reactor at different reactor geometry, packing material and operating conditions. The mass transfer model can further be incorporated into a biotic model that considers microbial growth and biofilm formation and be used as a tool for process design, optimization and up-scaling. Finally, the methodology presented in this study can be applied to other reactor types and processes that involve gases as substrates for microbial growth.

Declaration of Competing Interest

The authors declare that they have no known competing financial interests or personal relationships that could have appeared to influence the work reported in this paper.

Data availability

Data will be made available on request.

Acknowledgements

The authors would like to thank master student Marianna Krikeli for her assistance with the experimental work with the pilot reactor.

The work was financially supported by the Novo Nordisk Foundation within the framework of the Fermentation-based Biomanufacturing Initiative (FBM), grant number: NNF17SA0031362.

Appendix A. Supplementary data

Supplementary data to this article can be found online at <https://doi.org/10.1016/j.cej.2023.146086>.

References

- [1] H.N. Gavala, A. Grimalt-Alemany, K. Asimakopoulos, I.V. Skiadas, Gas Biological Conversions: The Potential of Syngas and Carbon Dioxide as Production Platforms, *Waste Biomass Valoriz.* 12 (10) (2021) 5303–5328.
- [2] A. Grimalt-Alemany, I.V. Skiadas, H.N. Gavala, Syngas biomethanation: state-of-the-art review and perspectives, *Biofuels, Bioproducts Biorefining.* 12 (1) (2018) 139–158.
- [3] K. Asimakopoulos, M. Kaufmann-Elfang, C. Lundholm-Höffner, N.B.K. Rasmussen, A. Grimalt-Alemany, H.N. Gavala, I.V. Skiadas, Scale up study of a thermophilic trickle bed reactor performing syngas biomethanation, *Appl. Energy* 290 (2021) 116771.
- [4] K. Asimakopoulos, M. Łężyk, A. Grimalt-Alemany, A. Melas, Z. Wen, H.N. Gavala, I. V. Skiadas, Temperature effects on syngas biomethanation performed in a trickle bed reactor, *Chem. Eng. J.* 393 (2020) 124739.
- [5] K. Asimakopoulos, H.N. Gavala, I.V. Skiadas, Biomethanation of Syngas by Enriched Mixed Anaerobic Consortia in Trickle Bed Reactors, *Waste Biomass Valoriz.* 11 (2) (2020) 495–512.
- [6] K. Asimakopoulos, H.N. Gavala, I.V. Skiadas, Reactor systems for syngas fermentation processes: A review, *Chem. Eng. J.* 348 (2018) 732–744.
- [7] B. Dahl Jønson, M. Ujarak Sieborg, M. Tahir Ashraf, L. Yde, J. Shin, S.G. Shin, J. Mi Triolo, Direct inoculation of a biotrickling filter for hydrogenotrophic methanogenesis, *Bioresour. Technol.* 318 (2020), <https://doi.org/10.1016/j.biortech.2020.124098>.
- [8] P.G. Kougias, P. Tsapekos, L. Treu, M. Kostoula, S. Campanaro, G. Lyberatos, I. Angelidaki, Biological CO₂ fixation in up-flow reactors via exogenous H₂ addition, *J. Biotechnol.* 319 (2020) 1–7.
- [9] T.L. Dupnock, M.A. Deshusses, High-Performance Biogas Upgrading Using a Biotrickling Filter and Hydrogenotrophic Methanogens, *Appl. Biochem. Biotechnol.* 183 (2) (2017) 488–502.
- [10] A. Azarpour, N. Rezaei, S. Zendejboudi, Performance analysis and modeling of catalytic trickle-bed reactors: a comprehensive review, *J. Ind. Eng. Chem.* 103 (2021) 1–41.
- [11] C. Feickert Fenske, F. Kirzeder, D. Strübing, K. Koch, Biogas upgrading in a pilot-scale trickle bed reactor – Long-term biological methanation under real application conditions, *Bioresour. Technol.* 376 (2023) 128868.

- [12] S. Paniagua, R. Lebrero, R. Muñoz, Syngas biomethanation: Current state and future perspectives, *Bioresour. Technol.* 358 (2022) 127436.
- [13] B.D. Jönson, P. Tsapekos, M. Tahir Ashraf, M. Jeppesen, J. Ejbye Schmidt, J.-R. Bastidas-Oyanedel, Pilot-scale study of biomethanation in biological trickle bed reactors converting impure CO₂ from a Full-scale biogas plant, *Bioresour. Technol.* 365 (2022) 128160.
- [14] S.D. Doig, K. Ortiz-Ochoa, J.M. Ward, F. Baganz, Characterization of Oxygen Transfer in Miniature and Lab-Scale Bubble Column Bioreactors and Comparison of Microbial Growth Performance Based on Constant kLa, *Biotechnol. Prog.* 21 (2008) 1175–1182, <https://doi.org/10.1021/bp050064j>.
- [15] W. Wu, S.G. Arhin, H. Sun, Z. Li, Z. Yang, G. Liu, W. Wang, Facilitated CO biomethanation by exogenous materials via inducing specific methanogenic pathways, *Chem. Eng. J.* 460 (2023), 141736, <https://doi.org/10.1016/j.cej.2023.141736>.
- [16] E.S. Gaddis, Mass transfer in gas–liquid contactors, *Chem. Eng. Process.* 38 (1999) 503–510, [https://doi.org/10.1016/S0255-2701\(99\)00046-X](https://doi.org/10.1016/S0255-2701(99)00046-X).
- [17] P.R. Gunjal, V.V. Ranade, R.V. Chaudhari, Liquid Distribution and RTD in Trickle Bed Reactors: Experiments and CFD Simulations, *Can. J. Chem. Eng.* 81 (3–4) (2003) 821–830.
- [18] B. Gunes, A critical review on biofilm-based reactor systems for enhanced syngas fermentation processes, *Renew. Sustain. Energy Rev.* 143 (2021) 110950.
- [19] K. Asimakopoulos, Biomethanation of synthesis gas in trickle bed reactors (Doctoral Thesis), Chapter 6 (189–190), Technical University of Denmark, 2019.
- [20] H. Porté, P.G. Kougias, N. Alfaro, L. Treu, S. Campanaro, I. Angelidaki, Process performance and microbial community structure in thermophilic trickling biofilter reactors for biogas upgrading, *Sci. Total Environ.* 655 (2019) 529–538.
- [21] M. Burkhardt, I. Jordan, S. Heinrich, J. Behrens, A. Ziesche, G. Busch, Long term and demand-oriented biocatalytic synthesis of highly concentrated methane in a trickle bed reactor, *Appl. Energy* 240 (2019) 818–826.
- [22] T. Ullrich, A. Lemmer, Performance enhancement of biological methanation with trickle bed reactors by liquid flow modulation, *GCB Bioenergy* 11 (1) (2019) 63–71.
- [23] T.L. Dupnock, M.A. Deshusses, Detailed investigations of dissolved hydrogen and hydrogen mass transfer in a biotrickling filter for upgrading biogas, *Bioresour. Technol.* 290 (2019) 121780.
- [24] K. Asimakopoulos, A. Grimalt-Alemany, C. Lundholm-Höfner, H.N. Gavala, I. V. Skiadas, Carbon Sequestration Through Syngas Biomethanation Coupled with H₂ Supply for a Clean Production of Natural Gas Grade Biomethane, *Waste Biomass Valoriz.* 12 (2021) 6005–6019, <https://doi.org/10.1007/s12649-021-01393-2>.
- [25] S.S. Riggs, T.J. Heindel, Measuring Carbon Monoxide Gas-Liquid Mass Transfer in a Stirred Tank Reactor for Syngas Fermentation, *Biotechnol. Prog.* 22 (2006) 903–906, <https://doi.org/10.1021/bp050352f>.
- [26] N. Jang, M. Lee, M. Yasin, I.S. Chang, Behavior of CO–water mass transfer coefficient in membrane sparger-integrated bubble column for synthesis gas fermentation, *Bioresour. Technol.* 311 (2020), 123594, <https://doi.org/10.1016/j.biortech.2020.123594>.
- [27] L. Rachbauer, G. Voitl, G. Bochmann, W. Fuchs, Biological biogas upgrading capacity of a hydrogenotrophic community in a trickle-bed reactor, *Appl. Energy* 180 (2016) 483–490, <https://doi.org/10.1016/j.apenergy.2016.07.109>.
- [28] C. Peintner, A.A. Zeidan, W. Schnitzhofer, Bioreactor systems for thermophilic fermentative hydrogen production: evaluation and comparison of appropriate systems, *J. Clean. Prod.* 18 (2010) S15–S22, <https://doi.org/10.1016/j.jclepro.2010.06.013>.
- [29] B.J. Azzopardi, R.F. Mudde, S. Lo, H. Morvan, Y. Yan, D. Zhao, *Hydrodynamics of Gas-Liquid Reactors*, Wiley (2011), <https://doi.org/10.1002/9781119970712>.
- [30] M.J. Ellman, N. Midoux, G. Wild, A. Laurent, J.C. Charpentier, A new, improved liquid hold-up correlation for trickle-bed reactors, *Chem. Eng. Sci.* 45 (7) (1990) 1677–1684.
- [31] A. Gianetto, V. Specchia, Trickle-bed reactors: state of art and perspectives, *Chem. Eng. Sci.* 47 (13–14) (1992) 3197–3213.
- [32] R. Knafe, P. Jacquinot, A.W.E. Hodgson, P.C. Hauser, Amperometric sensing in the gas-phase, *Anal. Chim. Acta* 549 (2005) 1–9, <https://doi.org/10.1016/j.aca.2005.06.007>.
- [33] J.R. Stetter, J. Li, Amperometric Gas Sensors A Review, *Chem. Rev.* 108 (2008) 352–366, <https://doi.org/10.1021/cr0681039>.
- [34] R.R. Zapico, P. Marín, F.V. Díez, S. Ordóñez, Liquid hold-up and gas–liquid mass transfer in an alumina open-cell foam, *Chem. Eng. Sci.* 143 (2016) 297–304, <https://doi.org/10.1016/j.ces.2016.01.008>.
- [35] A. Grimalt-Alemany, K. Asimakopoulos, I.V. Skiadas, H.N. Gavala, Modeling of syngas biomethanation and catabolic route control in mesophilic and thermophilic mixed microbial consortia, *Appl. Energy* 262 (2020) 114502.
- [36] W.G. Whitman, The two film theory of gas absorption, *Int. J. Heat Mass Transf.* 5 (5) (1962) 429–433.
- [37] P. Reichert, AQUASIM – A TOOL FOR SIMULATION AND DATA ANALYSIS OF AQUATIC SYSTEMS, *Water Sci. Technol.* 30 (2) (1994) 21–30.
- [38] D.J. Batstone, J. Keller, I. Angelidaki, S.V. Kalyuzhnyi, S.G. Pavlostathis, A. Rozzi, W.T.M. Sanders, H. Siegrist, V.A. Vavilin, The IWA Anaerobic Digestion Model No 1 (ADM1), *Water Sci. Technol.* 45 (2002) 65–73, <https://doi.org/10.2166/wst.2002.0292>.
- [39] R.A. Alberty, *Thermodynamics of biochemical reactions*, John Wiley & Sons, 2005.
- [40] W.M. Haynes, *CRC handbook of chemistry and physics*, CRC press, 2016.
- [41] G.S. Kell, Reanalysis of the density of liquid water in the range 0–150 °C and 0–1 kbar, *J. Chem. Phys.* 62 (1975). <https://doi.org/10.1063/1.430986>.
- [42] C.J. James, D.E. Mulcahy, B.J. Steel, Viscometer calibration standards: viscosities of water between 0 and 60 degrees C and of selected aqueous sucrose solutions at 25 degrees C from measurements with a flared capillary viscometer, *J. Phys. D Appl. Phys.* 17 (2) (1984) 225–230.
- [43] N.B. Vargaftik, B.N. Volkov, L.D. Voljak, International Tables of the Surface Tension of Water, *J. Phys. Chem. Ref. Data.* 12 (1983). <https://doi.org/10.1063/1.555688>.
- [44] D.F. Fairbanks, C.R. Wilke, Diffusion Coefficients in Multicomponent Gas Mixtures, *Ind. Eng. Chem.* 42 (3) (1950) 471–475.
- [45] J.L. Wise, G. Houghton, The diffusion coefficients of ten slightly soluble gases in water at 10–60°C, *Chem. Eng. Sci.* 21 (11) (1966) 999–1010.
- [46] D.L. Wise, G. Houghton, Diffusion coefficients of neon, krypton, xenon, carbon monoxide and nitric oxide in water at 10–60°C, *Chem. Eng. Sci.* 23 (10) (1968) 1211–1216.
- [47] W. Lu, H. Guo, I.M. Chou, R.C. Burruss, L. Li, Determination of diffusion coefficients of carbon dioxide in water between 268 and 473 K in a high-pressure capillary optical cell with in situ Raman spectroscopic measurements, *Geochim. Cosmochim. Acta* 115 (2013) 183–204.
- [48] J.J. Orgill, H.K. Atiyeh, M. Devarapalli, J.R. Phillips, R.S. Lewis, R.L. Huhnke, A comparison of mass transfer coefficients between trickle-bed, hollow fiber membrane and stirred tank reactors, *Bioresour. Technol.* 133 (2013) 340–346.
- [49] P. Harriott, A review of mass transfer to interfaces, *Can. J. Chem. Eng.* 40 (1962) 60–69, <https://doi.org/10.1002/cjce.5450400205>.
- [50] V.D. Mehta, M.M. Sharma, Effect of diffusivity on gas-side mass transfer coefficient, *Chem. Eng. Sci.* 21 (1966) 361–365, [https://doi.org/10.1016/0009-2509\(66\)85029-7](https://doi.org/10.1016/0009-2509(66)85029-7).
- [51] I. Iliuta, Faïçal Larachi, B.P.A. Grandjean, G. Wild, Gas–liquid interfacial mass transfer in trickle-bed reactors: state-of-the-art correlations, *Chem. Eng. Sci.* 54 (23) (1999) 5633–5645.
- [52] C. Wang, D.i. Song, F.A. Seibert, G.T. Rochelle, Dimensionless Models for Predicting the Effective Area, Liquid-Film, and Gas-Film Mass-Transfer Coefficients of Packing, *Ind. Eng. Chem. Res.* 55 (18) (2016) 5373–5384.
- [53] C.W. Green, J. Farone, J.K. Briley, R.B. Eldridge, R.A. Ketcham, B. Nightingale, Novel Application of X-ray Computed Tomography: Determination of Gas/Liquid Contact Area and Liquid Holdup in Structured Packing, *Ind. Eng. Chem. Res.* 46 (2007), <https://doi.org/10.1021/ie0701827>.
- [54] R.E. Tsai, P. Schultheiss, A. Kettner, J.C. Lewis, A.F. Seibert, R.B. Eldridge, G. T. Rochelle, Influence of Surface Tension on Effective Packing Area, *Ind. Eng. Chem. Res.* 47 (4) (2008) 1253–1260.
- [55] R.E. Tsai, A.F. Seibert, R.B. Eldridge, G.T. Rochelle, Influence of viscosity and surface tension on the effective mass transfer area of structured packing, *Energy Procedia* 1 (1) (2009) 1197–1204.
- [56] J.P. Cowger, K.T. Klasson, M.D. Ackerson, E. Clausen, J.L. Caddy, Mass-transfer and kinetic aspects in continuous bioreactors using *Rhodospirillum rubrum*, *Appl. Biochem. Biotechnol.* 34–35 (1992) 613–624, <https://doi.org/10.1007/BF02920582>.
- [57] M.H. Al-Dahhan, F. Larachi, M.P. Dudukovic, A. Laurent, High-Pressure Trickle-Bed Reactors: A Review, *Ind. Eng. Chem. Res.* 36 (1997) 3292–3314, <https://doi.org/10.1021/ie9700829>.
- [58] P.R. Gunjal, M.N. Kashid, V.V. Ranade, R.V. Chaudhari, Hydrodynamics of Trickle-Bed Reactors: Experiments and CFD Modeling, *Ind. Eng. Chem. Res.* 44 (2005) 6278–6294, <https://doi.org/10.1021/ie0491037>.
- [59] A. Kapic, S.T. Jones, T.J. Heindel, Carbon Monoxide Mass Transfer in a Syngas Mixture, *Ind. Eng. Chem. Res.* 45 (2006) 9150–9155, <https://doi.org/10.1021/ie060655u>.
- [60] N. Jang, M. Yasin, M. Lee, H. Kang, I.S. Chang, Gas circulation rate and medium exchange ratio as influential factors affecting ethanol production in carbon monoxide fermentation using a packed-bed reactor, *Sustain. Energy Fuels* 4 (2020) 1963–1973, <https://doi.org/10.1039/C9SE00943D>.
- [61] P.C. Munasinghe, S.K. Khanal, Syngas fermentation to biofuel: Evaluation of carbon monoxide mass transfer coefficient (kLa) in different reactor configurations, *Biotechnol. Prog.* 26 (2010) 1616–1621, <https://doi.org/10.1002/btpr.473>.
- [62] P.-H. Lee, S.-Q. Ni, S.-Y. Chang, S. Sung, S.-H. Kim, Enhancement of carbon monoxide mass transfer using an innovative external hollow fiber membrane (HFM) diffuser for syngas fermentation: Experimental studies and model development, *Chem. Eng. J.* 184 (2012) 268–277, <https://doi.org/10.1016/j.cej.2011.11.103>.
- [63] Y. Shen, R. Brown, Z. Wen, Syngas fermentation of *Clostridium carboxidivoran* P7 in a hollow fiber membrane biofilm reactor: Evaluating the mass transfer coefficient and ethanol production performance, *Biochem. Eng. J.* 85 (2014) 21–29, <https://doi.org/10.1016/j.bej.2014.01.010>.
- [64] K.T. Klasson, M.D. Ackerson, E.C. Clausen, J.L. Gaddy, Biodegradation of synthesis gas into liquid or gaseous fuels, *Enzyme Microb. Technol.* 14 (1992) 602–608, [https://doi.org/10.1016/0141-0229\(92\)90033-K](https://doi.org/10.1016/0141-0229(92)90033-K).
- [65] G. Wild, F. Larachi, J.C. Charpentier, Heat and mass transfer in gas-liquid-solid fixed bed reactors, in: M. Quintard, M.S. Todorovic (Eds.), *Heat and Mass Transfer in Porous Media*, Elsevier, Amsterdam, The Netherlands, 1992, pp. 616–632.
- [66] J. Zhang, A.R. Teixeira, K.F. Jensen, Automated measurements of gas-liquid mass transfer in micropacked bed reactors, *AIChE J.* 64 (2018) 564–570, <https://doi.org/10.1002/aic.15941>.
- [67] C. Wang, Y. Yang, Z. Huang, J. Sun, J. Wang, Y. Yang, B. Du, Gas-liquid mass transfer in a gas–liquid-solid three-phase moving bed, *Chem. Eng. J.* 420 (2021), 130449, <https://doi.org/10.1016/j.cej.2021.130449>.